Thesis for the degree of Doctor of Philosophy

# Making and identifying quantum resources

YU ZHENG


CHALMERS

Department of Microtechnology and Nanoscience (MC2)
*Applied Quantum Physics Laboratory*
Chalmers University of Technology
Göteborg, Sweden, 2023

Making and identifying quantum resources
YU ZHENG

ISBN 978-91-7905-919-4



Doktorsavhandlingar vid Chalmers tekniska högskola
Ny serie nr 5381
ISSN 0346-718X

Applied Quantum Physics Laboratory
Department of Microtechnology and Nanoscience (MC2)
Chalmers University of Technology
SE–412 58 Göteborg
Sweden
Telephone +46 (0)31 772 1000

Cover: Wigner function of a single-photon state.

Chalmers Digitaltryck
Göteborg, Sweden, 2023

Making and identifying quantum resources
YU ZHENG
Department of Microtechnology and Nanoscience (MC2)
Applied Quantum Physics Laboratory
Chalmers University of Technology

# Abstract

This thesis aims to investigate the properties of quantum systems that serve as valuable resources for information processing and their advantages over classical systems in specific tasks. While quantum computers have shown the ability to solve certain problems faster than classical computers, understanding the precise reasons behind this advantage remains a challenging task. The focus of this research lies in identifying and generating the quantum states that contribute to achieving quantum advantages.

The study begins by examining the distinctive characteristics of quantum systems in comparison to classical systems. Specifically, the thesis explores continuous-variable quantum computing, where quantum information is stored in continuous quantum variables. This stands in contrast to the more widely studied discrete-variable quantum processing in qubits. The investigation seeks to elucidate the potential of continuous-variable quantum computing and shed light on the specific states and operations that can provide quantum advantages.

The research explores the conversion of different quantum states through classical operations, investigating the feasibility of transforming tri-squeezed states into cubic phase states (Paper A), converting binomial states into resource states for universal quantum computing (Paper B), and creating two-photon states from single-photon states without single-photon detectors (Paper C). These studies reveal the possibility of achieving high-fidelity conversions with moderate success probabilities, uncovering valuable insights into the potential of these states as quantum resources.

Additionally, the thesis expands the research scope to encompass quantum advantage in random walks (Paper D). Random walks are fundamental to algorithms solving diverse computational problems, and the investigation aims to understand how quantum walkers can outperform classical walkers in certain scenarios. The analysis examines the behavior of quantum walkers, utilizing superposition states that occupy multiple nodes simultaneously. The study investigates the potential application of neural networks in identifying graph structures where quantum walkers exhibit advantages, with the goal of enhanc-

ing accuracy and understanding the underlying mechanisms.

By exploring the properties of quantum states and measurement techniques, this thesis contributes to a deeper understanding of quantum resources and advantages in computing.

**Keywords:** Quantum computing, continuous variables, universality, cubic phase state, photon number states, trisqueezed state, binomial states, Gottesman–Kitaev–Preskill states, Gaussian protocols, random walks, quantum walks, machine learning, neural networks, quantum advantage, quantum resources

# Acknowledgments

Would I go back and choose the PhD path again if given the chance? Absolutely.

I am grateful to my supervisor Anton Frisk Kockum and co-supervisor Giulia Ferrini, for their support, for the enormous space they give for understanding with heart. A special thank you goes to my examiner Göran Johansson. His leadership has cultivated an incredibly inclusive and nurturing working environment. I'm grateful to Fernando Quijandría and Alessandro Ferraro for all the inspiring discussions.

People I met at AQP are truly life gifts to me. I'm really grateful for each one of them.

Big kudos to Pontus Vikstål for showing me how to appreciate things as they naturally are. Also, thanks for introducing me to that game-changing documentary on factory farming without warning me of the consequences: you might just find myself becoming a veggie aficionado after watching it!

Major props to David Fitzek for loaning me that brain-bender of a book, "Gödel, Escher, Bach." And showing me how to cherish small moments for their pure existence.

A standing ovation for Hanna Linn and Ariadna Soro Álvarez, for showing being true to ourselves and responsible for the world we live in. Also thank you a lot for pushing me into the dance world led by the great teacher Phu! Whee!

Big thanks to Shahnawaz Ahmed for showing me the Gandhi-level kindness a person can have for anything. Seriously, if kindness was an Olympic sport, you'd be taking home gold while I'd still be struggling at the qualifiers!

In the end, I want to thank my parents for everything.

ps: The picture of two photons meeting in a beamsplitter helps me to understand what is a pure observation without any fixed picture or basis in mind.

pps: If you only read two pages, make it page 1, pages 24 (Chapter 4.4), and all the quotes. I'm always up for a chat about those sections!

Yu Zheng, Göteborg, September 2023

# Publications

**A** **Gaussian conversion protocols for cubic phase state generation**
Yu Zheng, Oliver Hahn, Pascal Stadler, Patric Holmvall, Fernando Quijandría, Alessandro Ferraro, and Giulia Ferrini
PRX Quantum **2**, 010327 (2021)

**B** **Gaussian conversion protocol for heralded generation of generalized Gottesman-Kitaev-Preskill states**
Yu Zheng, Anton Frisk Kockum, Alessandro Ferraro, and Giulia Ferrini
Physical Review A **108**, 012603 (2023)

**C** **Gaussian protocol for multi-mode states conversion**
Oliver Hahn, Patric Holmvall, Yu Zheng, Pascal Stadler, Giulia Ferrini, and Alessandro Ferraro
Manuscript in preparation (2023)

**D** **Detecting quantum speedup of random walks with machine learning**
Hanna Linn, Yu Zheng, and Anton Frisk Kockum
arXiv:2309.02212 (2023)

# Contents

# 1 Introduction

> Quantum physics: the only field where particles can teleport, spooky action is real, the only thing certain is the uncertainty, and scientists are okay with it!
>
> — ChatGPT

## 1.1 The essence of quantum physics

Quantum physics deals with the behavior of particles and energy at very small scales. What we can learn from quantum physics is quite profound and has implications for various aspects of understanding the universe. We can list a series of phenomena that occur in quantum mechanics and are counter-intuitive:

- **Observer effect**: The act of measuring a quantum system can change its state. This highlights the importance of the way of observation itself in physical processes.
- **Non-locality**: Quantum mechanics shows that particles can interact instantaneously over vast distances, which is known as quantum non-locality or "spooky action at a distance".
- **Wave-particle duality**: Quantum physics teaches us that particles can exhibit both wave-like and particle-like properties. This duality is at the heart of quantum mechanics and demonstrates the limitations of our classical understanding of the world.
- **Reality is probabilistic**: Quantum mechanics shows that reality is fundamentally probabilistic, not deterministic. Particles exist in a state of superposition, where they can be in multiple places or states simultaneously until they are measured.
- **Complementarity**: Quantum mechanics teaches us that some properties of particles are complementary, meaning that they cannot be measured simultaneously with complete accuracy.

After an in-depth exploration of quantum properties, our curiosity naturally leads us to the enigma of their real-world implications. These properties, rich in counter-intuitive behaviors, stand in stark contrast to classical physics and spark a fascinating proposition: could we harness these peculiarities for advanced computing [1] or other technologies, like quantum communication [2] and quantum sensing [3]? Such a prospect piques our interest not just in the mere possibility but in the practicality of it all. Given the quantum realm's bizarre and often elusive nature, one has to wonder about the quantum resources required to effectively tap into this potential. How might we quantify these resources [4]? And to what extent must we leverage them to achieve a significant edge over classical computational methods? As we stand at this crossroads of theoretical physics and practical computing, the journey ahead promises a confluence of challenges and revelations, pushing the boundaries of what we know and what we can achieve.

## 1.2 Approaches to quantum computing

There are generally two approaches to quantum information processing: one that encodes quantum information in systems with discrete variables (DVs) that have a finite number of degrees of freedom and another that encodes information in continuous variables (CVs) with an infinite number of degrees of freedom. Continuous-variable quantum systems are particularly promising for quantum computation due to their adaptability, and are the focus of this thesis.

In continuous-variable systems [5], quantum information is stored in wave functions of a continuous quantum variable. Continuous-variable quantum computation can be performed in a variety of physical settings, including optical systems [6], microwave radiation [7–10], trapped ions [11, 12], opto-mechanical systems [13–15], and atomic ensembles [16–19].

Significant advantages of CV systems include scalability [20–22], exemplified in the generation of one-million-mode cluster states [23], and noise resilience yielding a long lifetime of quantum information encoded in continuous variables [24].

Another attractive property of CV systems is the infinite Hilbert space that can be associated with a single bosonic mode. It means that quantum information can be encoded in a single bosonic mode to protect against errors at a logical level. One of the bosonic codes for suppression of logical errors, the Gottesman-Kitaev-Preskill (GKP) code [25, 26], has recently been experimentally achieved [27].

In addition to the well-studied DV and CV approaches, another notable approach to quantum computing is quantum walks [28]. Quantum walks form a unique intersection between CV systems and the dynamics of quantum mechanics. Classical random walks [29] have found widespread applications in algorithms [30–33], optimization, and statistical physics, and quantum walks are their quantum-mechanical counterparts, with even more fascinating and richer

dynamics.

In stark contrast to the somewhat predictable nature of classical walks, quantum walks leverage the principles of quantum superposition and interference, resulting in a walk that exhibits a different probability-distribution profile. This provides the potential for quantum advantage in the form of faster search algorithms and more efficient simulations [34].

A salient feature of quantum walks is their capability to perform universal quantum computation. This means that, in theory, any computational problem that can be addressed by a traditional quantum circuit can also be mapped onto a quantum walk framework [35–37]. This universality property of quantum walks expands the horizon for quantum computation overall, offering new paradigms for algorithm design and implementation.

Several experimental platforms, many of which overlap with the CV systems discussed earlier, have been employed to realize quantum walks [38–43]. Notably, optical systems are a prevalent choice, due to their inherent controllability and adaptability. The experimental demonstration of quantum walks in these systems stands as a testament to their practical relevance and potential.

## 1.3 Motivation for generating and identifying resource states

A critical question regarding these approaches to quantum computing is determining the resources needed to make CV quantum computers, or quantum random walks, more efficient than classical ones [44].

In CV systems, Gaussian processes correspond to bosonic interactions that are restricted to the second order of the position and momentum operators [45–47]. This implies that they are relatively easy to implement in many experimental platforms, but Gaussian operations alone cannot achieve computational universality [44]. This means that quantum non-Gaussianity is required as a resource [48, 49].

To promote Gaussian operations towards universal fault-tolerant quantum computation, one can, for example, introduce GKP states as the non-Gaussian resource [25, 50, 51], or introduce non-linearity through a cubic phase state [25, 52] to unlock universality regardless of the use of a specific encoding [44, 53].

In general, how a resource state can be obtained, starting from a non-Gaussian state via Gaussian protocols, has not been studied thoroughly yet. In this thesis, we will show feasible solutions to obtain non-Gaussian resource states that remain hard to achieve, by starting from non-Gaussian states that has been recently obtained experimentally. In Papers A, B, and C, we explore the dynamics of Gaussian protocols and the transformation pathways that enable the conversion of recently obtained experimental non-Gaussian states into viable non-Gaussian resources. By unveiling a coherent methodology and introducing novel techniques, we aspire to understand the intricate balance between Gaussian operations and non-Gaussian resources.

To better understand the necessary resources for quantum advantage, we also investigated, in Paper D, the conditions under which quantum walks can outperform classical random walks, a question for which analytical results exist only some types of graphs [54–64]. Specifically, we delve into the nuances of various graph structures—ranging from simple linear and cyclic graphs to more complex, irregular topologies. Additionally, the positioning of the initial and target nodes of the walks within these graph structures is another critical variable we examine. This aspect is particularly significant because the relative location of these nodes can drastically affect the efficiency and speed of both quantum and classical walks.

By exploring these details, we aim to draw broader parallels between the specific advantages observed in quantum walks and the general concept of quantum advantage in computing. Understanding these advantages in the context of simpler systems, like random walks on graphs, could provide valuable insights. These investigations serve as a microcosmic study that can help elucidate the more complex and overarching question: Under what conditions can quantum computing systems reliably outperform their classical counterparts?

## 1.4 Overview of the thesis

This thesis is dedicated to generating critical non-Gaussian resources, e.g., the GKP state, essential for universal quantum computation within CV quantum systems. We aim to study foundational tools pivotal to the field of CV quantum information. Understanding these elements can not only help us assess the current state of quantum information research, but also aid in mapping out its future directions.

In Chapter 2, we introduce the foundational concepts of CV quantum computing, with a focus on the significance of Gaussian operations and homodyne measurements. In Chapter 3, we present the resource states used as initial states and identify the target resource states, including photon states, tri-squeezed states, cubic phase states, as well as binomial and GKP states. In Chapter 4, we elucidate the general model and circuit architecture of the protocol employed for state conversion.

Moreover, this work aspires to demonstrate the practical application of machine learning in quantum systems. Specifically, we showcase a machine-learning method tailored to identify the quantum resources in continuous quantum walks.

To facilitate the understanding of Paper D, in Chapter 5, we delve into the dynamics of classical and quantum walks, drawing comparisons between the two through their implementations on a cyclic graph. This helps us understand how different types of walks behave in constrained environments. In Chapter 6, we dissect the architecture of neural networks by looking at their basic building blocks. We offer a comprehensive walkthrough that outlines the specific functionalities and roles of each component within the network.

In Chapter 7, we provide an overview of the key findings and contributions

of the appended papers, followed by a summary and future outlook in Chapter 8 to contextualize the research and suggest avenues for further study.

In essence, this thesis seeks to contribute valuable insights into both the theoretical aspects of continuous-variable quantum systems and quantum walks, particularly in relation to quantum computation and information processing.

# 2 Continuous-variable approach to quantum computation

> Particles, each described by a small finite number (six) of parameters (three positions and three momenta); and fields, requiring an infinite number of parameters. **At equilibrium, the energy is spread evenly among all the degrees of freedom of the system. Since the fields have infinitely many degrees of freedom, the poor particles get left with none at all.**
>
> — Roger Penrose, The emperor's new mind

Quantum computing is traditionally associated with qubits that corresponds to discrete two-level systems, e.g., the spin of an electron. However, recent improvements in experiments dealing with continuous variables in various platforms encourage the quantum-information community to also explore CV quantum computing [23, 24, 27, 65–67].

In this chapter, we will review the background of CV quantum computation starting from the quantized harmonic oscillator. This is followed by an introduction to general Gaussian operations in a CV quantum system. Then, we will show some important tools used in this thesis: position measurement and measurement-based gate teleportation. In the end, we will introduce Completely positive trace-preserving Gaussian maps.

## 2.1 The quantized harmonic oscillator

The concept of quantum implies that a physical property can be quantized. The first quantization method, canonical quantization, is established by expanding classical mechanics.

In quantum optics, the quantized electromagnetic modes correspond to quantum harmonic oscillators [68]. We begin with the classical Hamiltonian of a single-mode field, which is formally equivalent to a harmonic oscillator of unit mass:

$$H = \frac{1}{2}(p^2 + \omega^2 q^2), \tag{2.1}$$

where the real and imaginary parts of the quantized electromagnetic field play the roles of the canonical position $q$ and momentum $p$, and $\omega$ is the angular frequency of the oscillator [69].

The dynamics of classical systems is determined by the canonical Poisson brackets $\{q, p\}$. After Heisenberg found that one could not measure the momentum and position of a system simultaneously, Dirac made the connection with Poisson brackets [70]. The structure of the Poisson brackets is only partially preserved in canonical quantization as the commutator $[\hat{q}, \hat{p}]$ is equivalent to the Poisson bracket $\{q, p\}$ result multiplied by the constant $-\mathrm{i}\hbar$, where $\hbar$ is the reduced Planck constant.

It is convenient to introduce the definition of creation and annihilation operators as $\hat{a} = (\hat{q} + \mathrm{i}\hat{p})$ and $\hat{a}^\dagger = (\hat{q} - i\hat{p})$, which satisfy the bosonic commutation relation $[\hat{a}, \hat{a}^\dagger] = 1$. Note that here the convention is $\hbar = 1/2$, which we use in the rest of this thesis.

The vector of canonical coordinates operators for $N$ bosonic modes can be written as $\hat{\vec{r}} = (\hat{q}_1, \hat{p}_1 ... \hat{q}_N, \hat{p}_N)^T$, where $\hat{q}_i$ and $\hat{p}_i$ are the position and the momentum operators of the $i$th modes, respectively.

In CV systems, an important representation is the Wigner function, which is a quasiprobability distribution in phase space [71]:

$$W(q,p) = \frac{1}{h} \int \mathrm{e}^{-\mathrm{i}py/\hbar} \psi^*(q + y/2)\psi(q - y/2)\mathrm{d}y, \tag{2.2}$$

where

$$h = \frac{1}{\int\int W(q,p)^2 \mathrm{d}q\mathrm{d}p}. \tag{2.3}$$

Comparing with classical statistical mechanics where the Boltzmann factors contain energies, the factors are expressed as functions of both position $q$ and momentum $p$ in the Wigner function [71]. Because of the restriction of the uncertainty principle, it can shed light on the classical limit of quantum mechanics.

A pure state with positive Wigner function is a Gaussian state [72], whose wave function is an exponential function of a quadratic polynomial. Any quantum process can be simulated efficiently on a classical computer if it begins with Gaussian states, only performs transformations generated by Hamiltonians, and is followed by measurements also positively represented in terms of the Wigner function [73]. It has been proved that initial states or operations including measurements characterized by negative Wigner functions are necessary for quantum speed-up [74, 75]. Thus, Wigner negativity is a necessary resource for quantum advantage. Unlike the entanglement property, Wigner negativity is invariant under a change in the choice of basis.

To quantify the resource of a quantum state, one can calculate the Wigner logarithmic negativity, also known as *mana* [48, 76]

$$M(\rho) = \log\left( \int \mathrm{d}\vec{r} |W_\rho(\vec{r})| \right), \tag{2.4}$$

where $W_\rho(\vec{r})$ is the Wigner function of the state $\rho$, and where the integral runs over the whole phase-space.

## 2.2 Gaussian operations in continuous variables

The definition of quantum computing universality is that one can achieve any unitary transformation, with an arbitrarily fixed accuracy, stemming from Hamiltonians that are polynomial in the quadrature operators [44].

We can first recall the definition of Gaussian universality. Consider an operator $\hat{U}$ that is at most a quadratic polynomial in $\hat{q}$ and $\hat{p}$ (linear unitary Bogoliubov transformations). The evolution generated by $\hat{U}$ can then be characterized as [77]

$$\hat{U}^\dagger \hat{\vec{r}} \hat{U} = S\hat{\vec{r}} + \hat{\vec{c}}, \tag{2.5}$$

where $\hat{\vec{c}}$ is a displacement and $S$ is a symplectic matrix that satisfies $S\Omega S^T = \Omega$, and thus preserves the anti-symmetric symplectic form $\Omega$ under congruence [5], with

$$\Omega = \begin{bmatrix} I_n & 0 \\ 0 & -I_n \end{bmatrix}, \tag{2.6}$$

where $I_n$ is the $n \times n$ identity matrix.

Gaussian universality for a single mode can be attained with some basic operations in continuous-variable systems, for instance, the squeezing $\hat{S}(\xi)$, displacement $\hat{D}(\beta)$, and phase rotation $\hat{U}_p(\gamma)$ operators; see their definitions below.

- **Displacements:**

  A displacement in phase space is described by the displacement operator

  $$\hat{D}(\beta) = \mathrm{e}^{\beta \hat{a}^\dagger - \beta^* \hat{a}}, \tag{2.7}$$

  where $\hat{a}^\dagger$ and $\hat{a}$ are the creation and annihilation operators, respectively, and $\beta \in \mathbb{C}$ is a complex number that defines the magnitude and direction of the displacement. The displacement operator acts on a state to move it in phase space without changing its shape.

- **Squeezings:**

  Squeezing modifies the uncertainties in the complementary variables (quadratures) of the system. The squeezing operator is

  $$\hat{S}(\xi) = \mathrm{e}^{\frac{\xi^*}{2}\hat{a}^2 - \frac{\xi}{2}\hat{a}^{\dagger 2}}. \tag{2.8}$$

  Here, $\xi \in \mathbb{C}$ is the squeezing parameter. When this operator acts on a state, it will modify the uncertainties of the position and momentum (or the two quadratures in the case of light fields) such that the product of their uncertainties still respects the Heisenberg uncertainty principle.

- **Rotations:**

  A rotation in phase space is described by the operator

$$\hat{U}_p(\gamma) = \mathrm{e}^{-\mathrm{i}\gamma\hat{n}}, \tag{2.9}$$

  where $\gamma \in \mathbb{R}$ is the rotation angle and $\hat{n} = \hat{a}^\dagger\hat{a}$ is the number operator.

## 2.3 Universal operations in continuous variables

We know that Gaussian operators only allow the construction of any Hamiltonian that is quadratic in $\hat{q}$ and $\hat{p}$, and of no Hamiltonian of a higher order [44]. The latter can be achieved with the help of a non-Gaussian operation, for example, a cubic phase gate $\mathrm{e}^{\mathrm{i}r\hat{q}^3}$.

Given an input state, any unitary transformation can be achieved to an arbitrary degree of accuracy by some non-Gaussian operations combined with universal Gaussian operations on a single mode. Multi-mode universal transformations can be obtained by adding a two-mode Gaussian interaction, such as the $\hat{C}_Z$ gate [44, 78]

$$\hat{C}_Z = \mathrm{e}^{\mathrm{i}\hat{q}\otimes\hat{q}}. \tag{2.10}$$

Let us elucidate why Gaussian operators only permit the formulation of Hamiltonians quadratic in $\hat{q}$ and $\hat{p}$, while excluding the possibility of Hamiltonians of higher orders. In quantum mechanics, Gaussian operators are those that evolve the system via a linear combination of the position operators ($\hat{q}$) and momentum operators ($\hat{p}$), often accompanied by a displacement term. The term "Gaussian" often implies that the evolution of the state remains within the realm of Gaussian states, which are fully described by their first and second moments in $\hat{q}$ and $\hat{p}$. When we focus on Hamiltonians that are quadratic in $\hat{q}$ and $\hat{p}$, the equations of motion derived from the Schrödinger equation (or the Heisenberg equation) remain linear differential equations. This linearity ensures that Gaussian states evolve into Gaussian states, and it keeps mathematical manipulations relatively tractable.

Once higher-order terms are introduced into the Hamiltonian, these properties no longer hold. The resulting equations of motion become nonlinear differential equations, making the system significantly more complex to analyze. Moreover, higher-order Hamiltonians can evolve Gaussian states into non-Gaussian states, breaking the elegant properties associated with Gaussian operations.

When the Hamiltonian $H$ is quadratic in position and momentum, it takes a form that can usually be written as Eq. (2.1) with linear terms added to the right-hand side. Hamilton's equations of motion, derived from the Hamiltonian, are

$$\dot{q} = \frac{\partial H}{\partial p}, \quad \dot{p} = -\frac{\partial H}{\partial q}. \tag{2.11}$$

For a quadratic Hamiltonian, these partial derivatives will yield terms that are linear in $q$ and $p$. As a result, the equations of motion will be linear differential equations.

In summary, Gaussian operators allow for the construction of Hamiltonians that are quadratic in $\hat{q}$ and $\hat{p}$ because this ensures that the equations of motion are linear, tractable, and preserve the Gaussian nature of the initial states. Higher-order Hamiltonians introduce complexities that go beyond the scope of what Gaussian operators can handle.

## 2.4 Position measurement

In quantum systems, measuring the position of a particle is not just a passive act; it can fundamentally change the state of that particle. This ”collapse” of the quantum state allows us to know the particle's position with certainty, but at the same time, makes its momentum more uncertain due to the quantum rule known as the Heisenberg uncertainty principle.

This changing of a quantum state through measurement does not have to be detrimental — it can be useful. The idea is that by entangling a primary quantum system with an ancillary one and then measuring the position of the ancillary system, we can actually alter the state of the main quantum system in a useful way. Depending on the result of the position measurement, different operations can be applied to further steer the primary system into a desired state. Such ideas can be important for tasks like quantum computing. For example, we use such measurements in Papers A, B, and C, where we apply them in protocols for converting between states that are resources for quantum computing.

It is crucial to note, however, that while position measurements can be potent tools for state conversion, they also introduce randomness due to the probabilistic nature of quantum mechanics. Therefore, in practice, state conversion using position measurement often requires repetition, error correction, or post-selection to achieve high fidelity.

## 2.5 Measurement-based gate teleportation

Unlike the quantum gate array that expanded from the classical gate array and quantum random walks that are inherited from classical random walks, measurement-based quantum computing is a novel method [79] based on gate teleportation. This method for quantum computing makes use of measurements as discussed in Chapter 2.4; it was discovered by Gottesman and Chuang [80] to illustrate how entanglement can be used to reduce the resources needed in quantum circuits.

Let us look at this method by discussing how a cubic phase gate can be implemented with a cubic phase state, which is also a motivation for Paper A.

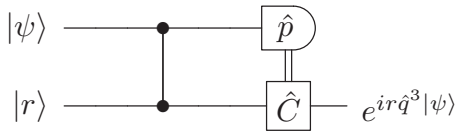


Figure 2.1: A gadget representing the cubic phase gate on an input state $|\psi\rangle$ implemented by means of the cubic-phase state $|r\rangle = e^{ir\hat{q}^3}\hat{S}(\xi)\,|0\rangle$, where $r$ is the cubic phase gate strength. $\hat{C}$ is a Gaussian correction. Figure adapted from Ref. [25].

As shown in Fig. 2.1, the control-$Z$ gate $\hat{C}_Z$ will entangle an arbitrary state $|\psi\rangle$ and a cubic phase state $|r\rangle$, which is defined as [52]

$$|r\rangle = e^{\mathrm{i}r\hat{q}^3}\hat{S}(\xi)\,|0\rangle\,, \tag{2.12}$$

where $\xi$ is the squeezing parameter, and $r$ yields the cubic interaction strength, called the *cubicity*.

By measuring the mode of the first rail in the $\hat{p}$ basis with outcome $m$, we obtain a state onto which has been applied a cubic phase gate after applying a Gaussian correction (rotation, displacing, or squeezing). The heart of this approach consists in transforming the resource from one state to another state with the help of measurement and entanglement operations.

## 2.6 Completely positive trace-preserving Gaussian maps

The unitary Gaussian transformations that we have defined above belong to the broad class of Gaussian maps. By adding the restrictions of such a map being a completely positive, trace-preserving linear map from density matrices to density matrices [5], a completely positive trace-preserving Gaussian transformation is defined. These maps are described by the symmetrically ordered characteristic function [45]

$$\chi_\rho(\hat{\vec{r}}) = \mathrm{Tr}\Big\{\hat{D}(-\hat{\vec{r}})\rho\Big\}, \tag{2.13}$$

with $\vec{r}$ the vector of canonical coordinates operator and the arbitrary displacement operator being

$$\hat{D}(-\hat{\vec{r}}) = \mathrm{e}^{-\mathrm{i}(\hat{\vec{r}}^T\Omega\hat{\vec{r}})}, \tag{2.14}$$

with $\hat{\vec{r}} \in \mathbb{R}^{2N}$ and $\Omega$ given in Eq. (2.6).

Any Gaussian completely positive trace-preserving map $\Phi$ on the characteristic function can then be written as [81]

$$\chi_\rho(\vec{r}) \to \chi_{\Phi(\rho)}(\vec{r}) = e^{-\frac{1}{4}\vec{r}^T\Omega^T Y\Omega\vec{r}+i\vec{l}^T\Omega\vec{r}}\chi_\rho(\Omega^T X^T\Omega\vec{r}), \tag{2.15}$$

with $X, Y$ being $2N \times 2N$ real matrices, $\vec{l}$ a $2N$ real vector, and $Y$ being symmetric and fulfilling the following positive semi-definite matrix constraint:

$$Y \pm i(\Omega - X\Omega X^T) \geq 0 \, . \tag{2.16}$$

The fidelity between a state $\rho$ and a target state $\rho_{\rm target}$, a measure which we use in several papers, can be defined in terms of characteristic functions:

$$\mathcal{F}(\rho, \rho_{\rm target}) = {\rm Tr}\{\rho\rho_{\rm target}\} = \frac{1}{4\pi} \int {\rm d}\hat{\vec{r}} \, \chi_\rho(\hat{\vec{r}}) \, \chi_{\rho_{\rm target}}(-\hat{\vec{r}}), \tag{2.17}$$

where $\chi_\rho$ and $\chi_{\rho_{\rm target}}$ are the characteristic functions of the states $\rho$ and $\rho_{\rm target}$, respectively.

# 3 Resource states

> A photon is a bosonic mode. You can keep shoving them into the same state, and they love it.
>
> — Frank Wilczek

This chapter is dedicated to an exploration of various resource states that we aim to convert between using Gaussian protocols. These resource states are all non-Gaussian states, i.e., they are characterized by a non-Gaussian Wigner function. As we noted in Chapter 1.3, non-Gaussian states or operations are required for achieving universal CV quantum computation, but Gaussian operations are usually easier to implement in experiments.

We begin by discussing the photon-number states, which we encounter in Paper C. These states serve as a straightforward starting point for understanding the resources at our disposal. Following that, we delve into more complex states, specifically, the trisqueezed states and cubic phase states, that are the focus of Paper A. These states are particularly interesting because they are connected to Hamiltonians that incorporate cubic terms. Finally, we shift our attention to binomial states and GKP states, as elaborated upon in Paper B. These states represent another layer of complexity in our study of resource states and offer unique opportunities for quantum computation and information processing.

At the outset, it is important to underscore the critical significance of the indistinguishability property for bosonic entities like photons. When two indistinguishable photons hit a beam splitter, we get a specific type of quantum interference where the photons ”stick together” and exit the beam splitter from the same port, and we cannot label one as “the photon that came in from the left” and the other as “the photon that came in from the right”. This is known as the Hong–Ou–Mandel effect [82]. The photons have to be identical in every measurable way — polarization, frequency, timing, etc. — for the interference to occur. For bosons, the wave function is symmetric under the exchange of particles, whereas for fermions, it is antisymmetric. These symmetries produce the observed statistical behaviors, leading to the vastly different properties and behaviors of bosons and fermions even though both are indistinguishable particles of their respective types.

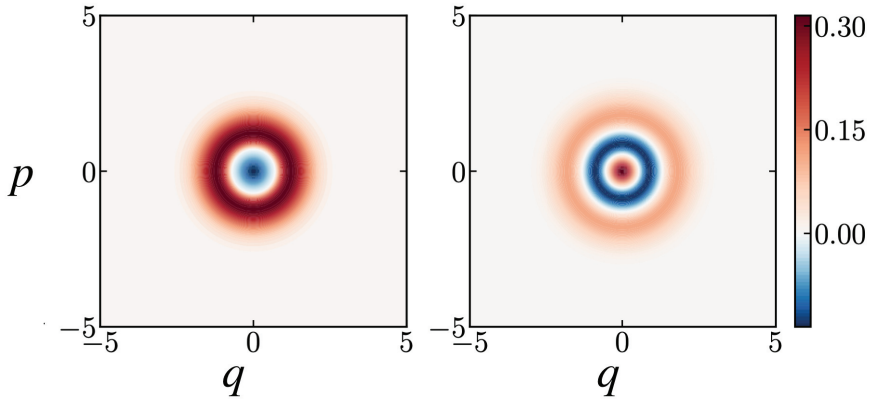


Figure 3.1: Wigner functions of (a) the one-photon state and (b) the two-photon state.

## 3.1 Photon number states

Photon number states embody the quantization of light, where the energy of electromagnetic radiation is quantized into discrete packets called photons. Figure 3.1 shows the Wigner functions of the one-photon state and the two-photon state. Any photon number state, often called Fock state, is orthogonal to Fock states with different photon numbers. The concept of photon number states highlights the particle-like nature of light and its fundamental quantum behavior. They allow for the precise measurement and counting of photons. Even the simplest single-photon states can exhibit remarkable interference effects, such as the famous double-slit experiment. When a single photon passes through a double-slit apparatus, it interferes with itself, creating an interference pattern that demonstrates the wave-particle duality of light.

A two-photon Fock state is a quantum state of light where exactly two photons are present in a single mode of the electromagnetic field. The two photons in the two-photon Fock state are indistinguishable, which leads to specific kinds of quantum interference effects, like the Hong–Ou–Mandel interference [82] (discussed above) when interacting with beam splitters, which is often considered a manifestation of the bosonic nature of photons. Creating an exact two-photon Fock state is experimentally challenging [83], but can be done using methods like parametric down-conversion (in a controlled manner), or through a single-photon source operated in a particular way to generate two photons [84]. These challenges motivate one conversion protocol, studied in Paper C, to create two-photon states.

## 3.2 The trisqueezed state

In this thesis, we address conversion protocols from experimentally available states to states that are known to be pivotal for quantum computation (see Chapter 1). The input state discussed in Paper A is the trisqueezed state, defined as [85, 86]

$$|\Psi_{\text{in}}\rangle = e^{i(t^*\hat{a}^3 + t\hat{a}^{\dagger 3})}|0\rangle\,. \tag{3.1}$$

In the ensuing discussion, we will use the term *triplicity*, denoted by the complex parameter $t$, to quantify the strength of the tri-photon interaction as represented in Eq. (3.1).

Figure 3.2(a) presents the Wigner function for a trisqueezed state characterized by a triplicity value of $t = 0.055$. This state exhibits several intriguing symmetries. First, it is symmetric with respect to the momentum axis $q = 0$. Secondly, the state possesses a $2\pi/3$-rotational symmetry. This rotational symmetry originates from the Hamiltonian that generates the state, as described in Eq. (3.1). This symmetry is also mirrored in the Fock-space expansion of the trisqueezed state, where only Fock states with photon numbers divisible by three are present [87]. This symmetry gives rise to a highly non-Gaussian Wigner function, exhibiting a distinct three-pointed star shape. The three arms of the star display triangular symmetry.

## 3.3 The cubic phase state

The cubic phase state is known for its significance in achieving universality in CV quantum computing [52]. It introduces nonlinear dynamics into the quantum realm, which in turn can enable powerful computational abilities beyond the scope of Gaussian states.

The wave function of a cubic phase state $|r\rangle$ from the definition in Eq. (2.12) can be computed by projecting into the position basis:

$$\Psi_{\text{target}}(q) = \langle q|\Psi_{\text{target}}\rangle = \left(\frac{2}{\pi}\right)^{\frac{1}{4}} e^{\xi_{\text{target}}/2} e^{-e^{2\xi_{\text{target}}}q^2} \mathrm{e}^{\mathrm{i}rq^3}, \tag{3.2}$$

where $\xi_{\text{target}}$ is the squeezing parameter of target cubic phase state and $r$ is the *cubicity*.

The distinctive feature of the cubic phase state is its phase shift, which is directly proportional to the cube of the position. This phase relationship introduces non-linear characteristics and non-Gaussian behavior into the quantum state.

From Fig. 3.2(b) we can see that the presence of quantum interference in a cubic phase state is evidenced by the nontrivial negative regions in its Wigner function [88]. These features underscore its utility as a valuable resource for quantum computing applications. Additionally, it is worth noting that the state exhibits symmetry with respect to the position axis, just as the trisqueezed state in Fig. 3.2(a).

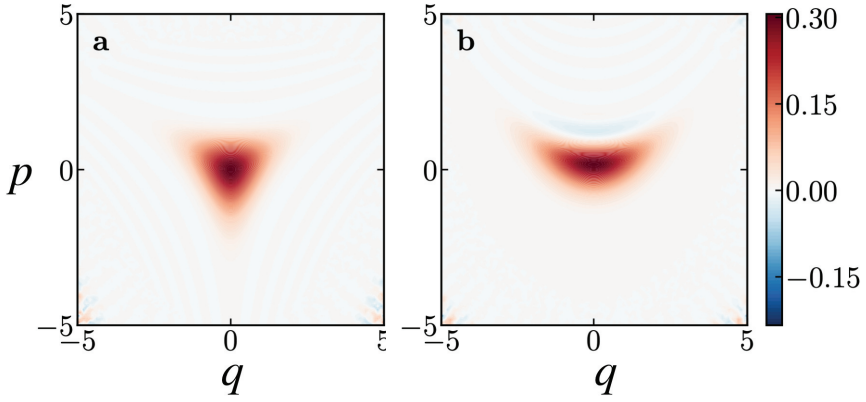


Figure 3.2: Wigner functions of (a) the trisqueezed state with triplicity $t = 0.055$ and (b) the target cubic phase state with squeezing parameter $\xi_{\text{target}} = 0.5$ and cubicity $r = 0.05$.

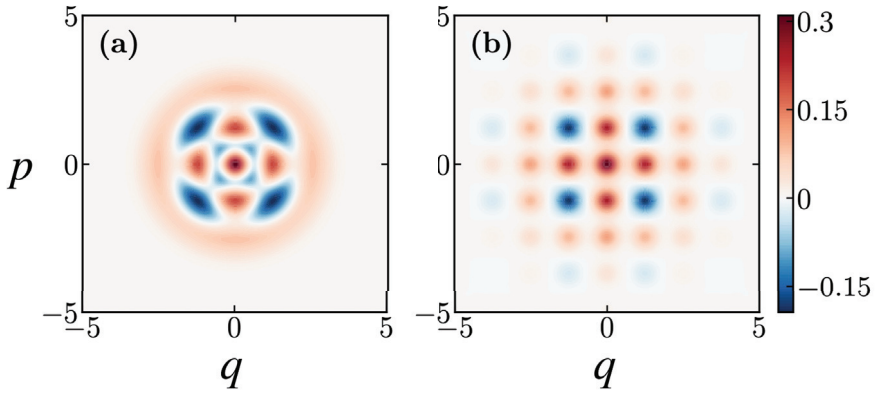


Figure 3.3: Wigner functions of (a) the binomial state with $N = 2$ and $K = 3$, and (b) the target qunaught state in Paper B, with 4.95 dB effective squeezing.

## 3.4 Binomial states

The binomial and Gottesman–Kitaev–Preskill (GKP) states are quintessential examples of non-Gaussian states that play pivotal roles within the realm of continuous-variable quantum computing [10, 89–91].

The binomial states, as the name suggests, find their roots in the binomial theorem. They are superpositions of Fock states with binomially distributed photon numbers, and can be used in quantum error correction codes. In the family of $N$-fold binomial codes, the 0-logical code-word is mathematically defined as [89, 92]

$$|0_N\rangle = \sum_{k=0}^{\lfloor K/2 \rfloor} \sqrt{\frac{1}{2^{K-1}} \binom{K}{2k}} \, |2kN\rangle \,, \tag{3.3}$$

where $\lfloor K/2 \rfloor$ is the floor function of $K/2$ and $K$ serves as the truncation param-

eter to limit the sum. The term $N$ represents the order of rotation symmetry, meaning that the state remains unchanged when rotated by an angle of $\pi/N$. This rotational symmetry lends the state useful properties for specific quantum protocols.

As an illustration, let us consider a specific example with parameter values $K = 3$ and $N = 2$, which was the focus of Paper B:

$$|\psi_0\rangle \equiv |0_2\rangle = \frac{1}{2}|0\rangle + \frac{\sqrt{3}}{2}|4\rangle\,. \tag{3.4}$$

Here, the state $|\psi_0\rangle$ emerges as a weighted superposition of $|0\rangle$ and $|4\rangle$, with the weights determined by the binomial coefficient for $K = 3$ and the order of rotational symmetry, which can be observed in Fig. 3.3(a).

## 3.5 Gottesman–Kitaev–Preskill states

Gottesman–Kitaev–Preskill (GKP) states [90] are named after their discoverers, Daniel Gottesman, Alexei Kitaev, and John Preskill. These states are designed to serve as a bridge between discrete-variable and continuous-variable quantum computing by encoding qubits in infinite-dimensional harmonic oscillator systems. The canonical GKP state, or sensor state, can be used as a tool for detecting minuscule displacements in phase space [93]. It is formally defined by the equation [90]

$$|\psi\rangle \propto \sum_{t=-\infty}^{\infty} e^{-\pi\Delta^2 t^2}\hat{D}(t\sqrt{\pi})\hat{S}(\Delta)\,|0\rangle\,, \tag{3.5}$$

In this equation, the operator $\hat{S}(\Delta)$ represents squeezing [cf. Eq. (2.8)], which transforms $\hat{q}$ into $\hat{q}\Delta$ and $\hat{p}$ into $\hat{p}/\Delta$, and $\hat{D}(\beta)$ is the displacement operator [cf. Eq. (2.7)]. An example of a qunaught state, the target of the conversion protocol in Paper B, is shown in Fig. 3.3(b).

The GKP states serve as a remarkable exception to the usual implications of the Heisenberg uncertainty principle, which constrains simultaneous precision in complementary variables like position ($\hat{q}$) and momentum ($\hat{p}$). Specifically, GKP states are crafted to be approximate eigenstates of both $\hat{q}$ and $\hat{p}$, modulo some integer multiples of $\sqrt{\pi}$, thereby subverting the naive interpretation of the uncertainty principle. Additional interesting properties of GKP states are

- **Quasi-classical behavior**: In a classical sense, specifying a state with near-simultaneous precision in $\hat{q}$ and $\hat{p}$ is equivalent to pinpointing a point in phase space. GKP states achieve a quantum version of this by localizing around lattice points in phase space.

- **Quantum robustness**: Despite this quasi-classical localization, GKP states maintain inherent quantum features, such as superposition. These quantum properties make them suitable for quantum error correction, which requires the manipulation of quantum states.

- **Built-in fault tolerance**: The lattice structure in phase space renders GKP states inherently robust against small Gaussian noise and displacements, which are common types of errors in CV quantum systems. This fault-tolerant nature is crucial for practical quantum computation, as it reduces the overhead for additional error correction.
- **Bridge to universal quantum computing**: Their resilience to specific errors and their capability to approximate forbidden eigenstates make GKP states an invaluable resource for constructing more sophisticated error-correcting codes. This feature paves the way for their use in universal quantum computing schemes.

In summary, GKP states occupy a unique niche in the quantum state space, blending classical-like determinism with quantum flexibility and robustness, thereby offering a promising avenue for fault-tolerant quantum computation.

# 4 Gaussian conversion protocols

> Quantum circuits are the brushstrokes of the quantum artist, painting a canvas of entanglement and uncertainty. They reveal the intricate dance of particles, challenging our intuitions and inviting us to explore the mysteries of the quantum realm.
>
> — Alain Aspect

In Papers A, B, and C, we explore the relationship between different families of quantum codes and states by leveraging transformations between distinct bases. One example (Paper B) is the generation of GKP codes (see Chapter 3.5), translationally symmetric codes, from binomial codes (see Chapter 3.4), which are rotationally symmetric codes. Other examples are conversion protocols going from multiple copies of one non-Gaussian resource state to one copy of another non-Gaussian resource state (Paper C) and the generation of the cubic phase state from a trisqueezed state (Paper A). In the last example, the trisqueezed state involves cubic powers of the creation and annihilation operators $\hat{a}^\dagger$ and $\hat{a}$. The cubic phase state is characterized by a phase term the cube of the position $\hat{a}^3$. Both states involve the cube of an operator or position variable, demonstrating their non-linear relationship with the photon number or position. Two key transformations in the protocol govern the relationship between the initial and target states.

The first transformation involves the relationship between the Fock basis and the position basis. This basis change has some connection to the wave-particle duality of quantum systems. In the Fock basis, we describe the states in terms of photon numbers, representing the energy levels of the quantum harmonic oscillator. Conversely, the position basis characterizes states through electric field amplitudes, offering a spatial interpretation of the system. Within our protocols, the focus predominantly rests on the position basis, and with good reason. By subjecting the system to measurements in a position basis, a transformation unfolds. The quantum state elegantly condenses into a position eigenstate, corresponding to a particular position within the spatial domain. Spatial stabilization can thus be implemented through this measurement.

The second crucial operation involves the transformation between the momentum basis and the position basis in the measurement, encapsulating the essence of the Heisenberg uncertainty principle. In quantum mechanics, the position and momentum of a particle are represented by non-commutative operators, resulting in this uncertainty principle, which imposes a trade-off between precise knowledge of both properties simultaneously. By implementing measurements in both the momentum and position directions in a sequence of circuits, we achieve a symmetry of uncertainty in both basis, especially when targeting symmetrical states like the GKP state.

In Papers A, B, and C, we thus explore the intricate connections between diverse families of quantum codes and states while making connections to foundational concepts in quantum mechanics, such as wave-particle duality and the Heisenberg uncertainty principle. In the subsequent sections of this chapter, we detail three specific quantum circuits integral to our resource-state conversion protocols in these three papers. While these circuits exhibit interdependencies, each provides distinct advantages tailored to optimize the conversion process in individual scenarios.

## 4.1 General considerations

The utilization of beamsplitters and position detection in quantum state generation unveils a captivating interplay between fundamental quantum phenomena and ingenious experimental techniques.

Beamsplitters, represented by unitary operators, facilitate the controlled splitting and recombination of quantum states. Their inherent ability to distribute quantum information across multiple paths enables the creation of intricate superpositions, a cornerstone of quantum computing and communication.

Position detection (see Chapter 2.4), on the other hand, brings the ethereal concept of wavefunction collapse into tangible reality. By measuring the position of a quantum particle, the probabilistic nature of quantum states manifests itself. The outcome of a position measurement collapses the wavefunction onto a specific position eigenstate, yielding information about the particle's spatial distribution.

Beamsplitters create intricate quantum superpositions, while position detection transforms abstract probability amplitudes into concrete spatial information. The use of two input states and beam splitters highlights the importance of quantum interference and entanglement in state generation, showcasing the application of quantum effects in generating valuable quantum resources.

## 4.2 Circuit for generating cubic phase states

In this section, we will show a protocol, from Paper A, for generating cubic phase states (see Chapter 3.3), characterized by a phase shift proportional to the cube

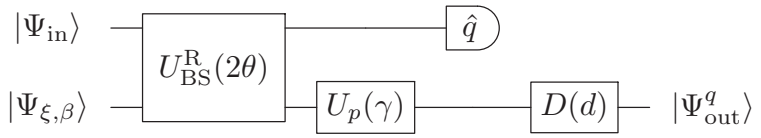


Figure 4.1: The circuit of our probabilistic Gaussian conversion protocol in Paper A. We start from two states and mix them in a beam-splitter $U_{\text{BS}}^{\text{R}}(2\theta)$. After a rotation $U_p(\gamma)$, we post-select the homodyne measurement on the first mode to value $q = 0$ and displace the second mode with $D(d)$.

of the position variable. This will be achieved starting from a trisqueezed state (see Chapter 3.2), which itself involves the cube of the photon position operator.

As sketched in Fig. 4.1, our conversion protocol takes two states as input, which include non-Gaussian resources and are similar to the target states but easier to achieve in general in experiments. These are mixed by a beam-splitter corresponding to the symplectic transformation

$$U_{\text{BS}}^{\text{R}}(2\theta) = \begin{pmatrix} \cos\theta & \sin\theta \\ -\sin\theta & \cos\theta \end{pmatrix}. \tag{4.1}$$

The next step is to perform a phase rotation on the lower rail, and that is followed by a homodyne measurement. We post-select the result $q = 0$ on the upper rail and apply a displacement on the state on the lower rail in the end when it is necessary.

Let us calculate explicitly the output state of the circuit sketched in Fig. 4.2. To simplify the calculation, we consider the output state before the displacement as it is equivalent to displacing the target state in terms of fidelity. The output state, which corresponds to an ideal measurement outcome $q$, is expressed as

$$\begin{aligned} |\Psi_{\text{out}}^q(\xi,\beta,\theta,\gamma)\rangle = &\frac{1}{\pi}\int \mathrm{d}q_2\ d\alpha \Psi_{\text{in}}(q\cos\theta + q_2\sin\theta) \\ &\Psi_{\xi,\beta}(-q\sin\theta + q_2\cos\theta)\langle\alpha|q_2\rangle|\alpha e^{-i\gamma}\rangle, \end{aligned} \tag{4.2}$$

where the squeezing parameter $\xi$ and the displacement $\beta \equiv q_\beta + ip_\beta$ are complex numbers, while the angle $\theta$ of the beam-splitter and the phase rotation $\gamma$ are real numbers.

## 4.3 Circuit for generating Gottesman–Kitaev–Preskill states

In this section, we introduce a protocol for generating Gottesman-Kitaev-Preskill (GKP) states (see Chapter 3.5), known for their translational symmetry, from binomial states (see Chapter 3.4) characterized by rotational symmetry. We detail an iterative procedure to transform between these two types of quantum

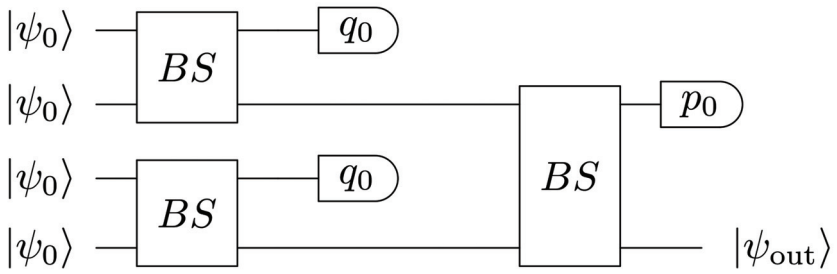


Figure 4.2: Sketch of our Gaussian conversion protocol with two iterations. Two binomial states $|\Psi_0\rangle$ are combined in a real balanced (50:50) beam-splitter. We then use a homodyne detector to measure the first modes' $\hat{q}$ quadrature. In the second iteration, we instead measure the $\hat{p}$ quadrature of one of the beam-splitter outputs.

codes—specifically, GKP states and four-fold symmetric binomial states that encode a zero-logical qubit—utilizing solely Gaussian operations.

Our iterative conversion protocol for transforming initial binomial states into the target qunaught state is inspired by the breeding protocol outlined in Ref. [94]. Unlike the original approach, which starts from squeezed cat states, our method commences with binomial states as delineated in Eq. (3.4). Additionally, we adopt a strategy of alternating measurements in the position ($\hat{q}$) and momentum ($\hat{p}$) quadratures.

The circuit depicted in Figure 4.2 implements two cycles of our conversion protocol. In the initial cycle, two pairs of binomial input states $|\psi_0\rangle$ are entangled through real balanced beam-splitters, followed by measurements of the $\hat{q}$ quadrature on the first modes. The resulting state of the second mode from each beam-splitter serves as the input for the next cycle. Each $\hat{q}$ and $\hat{p}$ measurement induces a squeezing effect on the output state in the respective quadratures. To equalize the squeezing strength in both directions, the second cycle incorporates a $\hat{p}$ measurement.

## 4.4 Generating two-photon states with homodyne detection

In Paper C, we investigate protocols converting multiple copies of resource states into another resource state. Here, we focus on the particular case of one- and two-photon states (see Chapter 3.1). It is well known that a beam-splitter can be used to mix two excited modes. If we initially have one photon in each of the input modes, the state $|1,1\rangle$, then the state after the beam splitter is a superposition of two photons propagating together in one of the mode [82]. The

two photons are bunched in the same mode after the beam-splitter:

$$|\Psi_{\text{out}}\rangle = \frac{1}{\sqrt{2}}\left(|2,0\rangle + |0,2\rangle\right). \tag{4.3}$$

It is very obvious that we in this way can obtain a two-photon state with photon detection (a non-Gaussian operation). But what if we use a position measurement (a Gaussian operation) instead?

Let us consider photon-number states in the $\hat{q}$ basis to explore the spatial distribution and quantum interference effects of these states. This analysis helps understand how the displacement parameter $d$ affects the spatial behavior of the single photons and how correlations between the two copies of the states manifest in position space.

First, we have two copies of displaced single-photon states $\psi_1(q+d)$ and $\psi_2(q-d)$. These states can be written in the $\hat{q}$ basis as follows [83]:

$$\psi_1(q_1+d) = 2\left(\frac{2}{\pi}\right)^{\frac{1}{4}} e^{-(q_1+d)^2}(q_1+d), \tag{4.4}$$

$$\psi_2(q_2-d) = 2\left(\frac{2}{\pi}\right)^{\frac{1}{4}} e^{-(q_2-d)^2}(q_2-d). \tag{4.5}$$

Then, $\psi_1(q_1+d)$ and $\psi_2(q_2-d)$ are fed into the real balanced beam-splitter. The two-mode output state can be written as (ignoring normalization)

$$\begin{aligned}
|\psi_{12}\rangle &\propto \int dq_1 dq_2 \psi_1(q_1\cos\theta + q_2\sin\theta)\psi_2(-q_1\sin\theta + q_2\cos\theta)\,|q_1\rangle\,|q_2\rangle \\
&\propto \int dq_1 dq_2 e^{-(\frac{\sqrt{2}}{2}(q_1+q_2+d))^2} \\
&\quad \left[\frac{\sqrt{2}}{2}(q_1+q_2+d)\right] e^{-(\frac{\sqrt{2}}{2}(-q_1+q_2-d))^2}\left[\frac{\sqrt{2}}{2}(-q_1+q_2-d)\right]|q_1\rangle\,|q_2\rangle\,.
\end{aligned} \tag{4.6}$$

We do a homodyne detection on the first mode and post-select the case when $q_1 = 0$. The output state can then be written as

$$\begin{aligned}
\langle q_1=0|\psi_{12}\rangle &= \int dq_1 dq_2 \psi_{12}(q_1,q_2)\,\langle q_1=0|q_1\rangle\,|q_2\rangle \\
&\propto \int dq_2 e^{-\frac{(q_2+d)^2}{2}} e^{-\frac{(q_2-d)^2}{2}} \frac{(q_2+d)(q_2-d)}{2}\,|q_2\rangle \\
&\propto \int dq_2 \frac{1}{2} e^{-q_2^2-d^2}(q_2^2-d^2)\,|q_2\rangle \\
&\propto \int dq_2 \frac{1}{2} e^{-q_2^2}(q_2^2-d^2)\,|q_2\rangle
\end{aligned} \tag{4.7}$$

The two-photon states can be written in q basis as

$$\psi_1(q) \propto e^{-q^2}\left(q^2 - \frac{1}{4}\right). \tag{4.8}$$

We can see that when $d = \frac{1}{2}$, the output state of Eq. (4.7) will be a two-photon state. We also perform numerical simulations to validate this state-generation protocol. The result shows perfect agreement with the analytical calculation. With these displacements, the interference of two states will generate an output state with 0.1077 probability and 0.99999 fidelity to the two-photon state.

# 5 Classical and quantum random walks

In the preceding chapters, our discussions have revolved around Gaussian operations and their interplay with non-Gaussian resources, but in this thesis, we wish to address a broader context of quantum advantage. Specifically, what conditions must be satisfied for quantum systems to outperform classical systems in computational tasks?

To this end, this chapter introduces the concept of quantum walks, which serve as an enlightening probe into the nature of quantum advantage. Quantum walks are the quantum analogs of classical random walks, and they can offer performance benefits over their classical counterparts under certain conditions, as we study in Paper D. But what are these conditions? And how do they relate to the more general query of quantum advantage in quantum computing?

This chapter aims to provide a comprehensive understanding of random walks, beginning with an exploration of classical random walks. Following this, we introduce the concept of quantum walks as a quantum analog to the classical version. Our investigation culminates in a comparative analysis of both classical and quantum walks on a simple cyclic graph.

## 5.1 Classical random walks

Random walks on graphs serve as a vital link between discrete mathematics and probabilistic studies, extending their influence well beyond abstract theory [95]. Starting from a specific vertex, the walker traverses the graph, adhering to a uniform probability distribution [96].

We consider an undirected graph $G = (V, E)$, where $V$ is the set of vertices and $E$ is the set of edges. The graph is represented by its adjacency matrix $A$ of dimensions $n \times n$, where $n = |V|$.

A particle starts its walk at the initial node $i = 0$ and aims to reach the target node $i = 1$. The particle is allowed to move from node $i$ to node $j$ if and only if $A_{ij} = 1$. To ensure that the particle remains at the target node upon reaching it, we introduce a self-loop by setting $A_{11} = 1$.

The master equation governing the continuous-time random walk (CTRW) in this setup is given by

$$\frac{dp_i(t)}{dt} = (T_{ij} - I)p_i(t), \tag{5.1}$$

with $p_i(t)$ the probability of being in node $i$ at time $t$ and $T_{ij}$ defined as

$$T_{ij} = \frac{A_{ij}}{d(j)}, \tag{5.2}$$

where $d(j)$ is the degree of node $j$ [97, 98].

One goal in the study of random walks is to find the "hitting time," which is defined as the time $t$ at which the particle first reaches the target node. Specifically, for the mean hitting time, we look for the time step $\tau$ at which the probability $p(\text{target}, \tau)$ exceeds a predefined threshold $p_{th}$, i.e.,

$$p(\text{target}, \tau) > p_{th}. \tag{5.3}$$

For random graphs, the characteristic path length scales with $\log n$, which informs the choice of $p_{th}$ [99].

## 5.2 Continuous-Time quantum walk

Quantum walks extend the concept of classical random walks into the quantum realm. Just like a classical walk is described by a probability distribution, a quantum walk is characterized by a quantum state that evolves over time according to the rules of quantum mechanics.

Here, we describe a continuous-time quantum walk (CTQW) on the same graph $G = (V, E)$, but extend the Hilbert space to include a "sink" node. This auxiliary node is used to trap and detect the quantum particle in the target node without collapsing its wave function [100]. We denote the modified adjacency matrix, with the sink node included, by $A^q_{ij}$.

The dynamics of the CTQW can be described using the Lindbladian equation for the density matrix $\rho$:

$$\frac{d\rho(t)}{dt} = -\frac{i}{\hbar}[\hat{H}, \rho(t)] + \gamma(L\rho(t)L^\dagger - \frac{1}{2}\{L^\dagger L, \rho(t)\}), \tag{5.4}$$

where $L = |\text{sink}\rangle \langle\text{target}|$ is the jump operator, dictating the decay from the target to the sink node with rate $\gamma$, and $\hat{H} = \hbar A^q_{ij}$ serves as the Hamiltonian [101].

Similar to the classical case, we are interested in the mean hitting time of the quantum walk, defined as the time $\tau$ when the probability of finding the particle in the sink node exceeds $p_{th}$, i.e.,

$$\rho_{\text{sink, sink}}(\tau) > p_{th}. \tag{5.5}$$

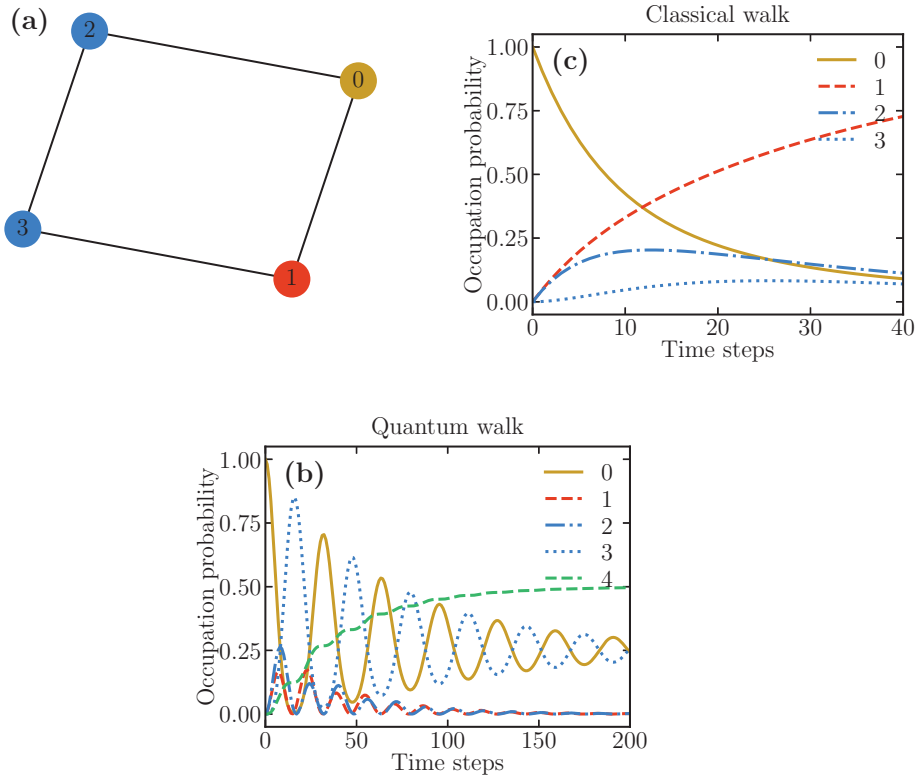


Figure 5.1: (a) A four-node cyclic graph with the initial node 0 in yellow, the target node 1 in red, and other nodes in blue. (b) Dynamics of a classical walk on this graph. (c) Dynamics of a quantum walk on the same graph. The green dashed line shows the population of the sink node 4, which is connected to the target node.

## 5.3 Classical and quantum walks on a cycle

Examining the distinctions between classical and quantum continuous walks on simple cyclic graphs is not only intriguing, but also opens a window into the subtleties of quantum phenomena, particularly in terms of hitting times. A simple cyclic graph consists of a closed loop of $n$ nodes, where each node is connected to its immediate neighbors. This structured setting provides an excellent backdrop to explore whether quantum walks outperform classical walks in the realm of hitting times.

Figure 5.1 visually illustrates these concepts. In classical walks, the probability distribution of the particle evolves naturally, free from interference between different paths. The quantum realm is markedly different: due to the interference of quantum states, the resulting probability distribution showcases a complex landscape of peaks and valleys.

This brings us to an essential aspect of quantum walks: the introduction of “dark” and “bright” states within the Hilbert space. A “dark” state is a

quantum state that remains undetected due to destructive interference effects. Conversely, "bright" states are those that are orthogonal to the dark space and are always detected. The presence of a detector partitions the entire Hilbert space into these two mutually exclusive sectors.

The probability of detection in the limit of long time, denoted as $P_{\text{det}}$, can be understood as the overlap between the initial state and the bright space. This overlap can be further constrained by considering the number of states that are "equivalent" in terms of their detectability. Mathematically, this constraint manifests as an upper bound on $P_{\text{det}}$, given by the inverse of the number of equivalent states. The more equivalent states present, the lower the upper bound becomes, serving as a metric for the challenge inherent in detecting a specific state.

Cyclic graphs demonstrate unique behavior based on their nodal count. For graphs with an odd number of nodes, $P_{\text{det}}$ remains a constant $\frac{1}{2}$. In even-numbered graphs, a notable exception arises: at the node diametrically opposite to the target, $P_{\text{det}}$ reaches unity, guaranteeing the detection of the desired state.

In the four-node cyclic graph of Fig. 5.1, the total detection probability is $\frac{1}{2}$ due to symmetry. However, quantum walks show oscillatory behavior between symmetric initial nodes, eventually leading to energy localization in the target node (which leaks into the sink node) and in a superposition of nodes 0 and 3, which are symmetric with respect to the target node [Fig. 5.1(c)].

# 6 Neural networks

Identifying instances where quantum walks genuinely offer a speedup over their classical counterparts remains a complex task. It involves intricate analysis and simulations that often become infeasible due to computational limitations. This raises an inevitable question: Can we use machine learning, specifically neural networks, to predict or even discover the scenarios where quantum walks exhibit a speedup? In this chapter, we delve into the biological inspirations and historical background of neural networks, explore various activation functions, and discuss critical learning rules. By doing so, we lay the groundwork for employing neural networks as a robust tool to shed light on the elusive question of quantum speedup in quantum walks, as we do in Paper D.

## 6.1 Biological inspiration and history

In 1943, Warren McCulloch and Walter Pitts published a seminal paper [102] that proposed a mathematical model for artificial neurons, which transmit information through electrical and chemical signals. To bridge the gap between neuroscience and computational models, the McCulloch-Pitts model simplified the complex structure of biological neurons, representing them as binary threshold units that receive input, process it, and generate an output. It can perform basic logical operations such as AND, OR, and NOT, which are essential building blocks of digital computing. This capability demonstrated that artificial neural networks could be used to replicate complex decision-making processes and perform computations. The model is Turing-complete as it can compute any computable function given enough neurons and an appropriate configuration. This universality established the potential of artificial neural networks as general-purpose computational models.

In 1958, Frank Rosenblatt [103] introduced the perceptron, an early type of artificial neural network. The perceptron was designed as a single-layer network that could learn to classify linearly separable patterns, where all data points belonging to the same category or class lie on the same side of a dividing line, plane, or hyperplane, through a process of supervised learning which is trained on a labeled data set.

The backpropagation algorithm, popularized by David Rumelhart, Geoffrey

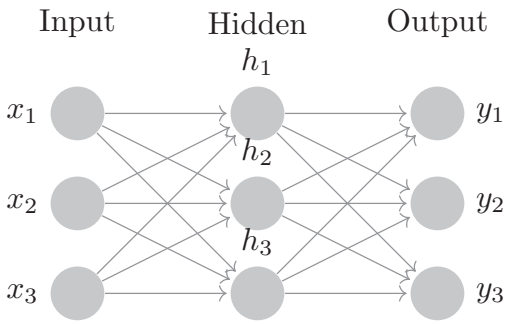


Figure 6.1: Illustration of a feedforward neural network with annotated neurons. The input layer neurons are denoted $x_1, x_2, x_3$, the hidden layer neurons are $h_1, h_2, h_3$, and the output layer neurons are $y_1, y_2, y_3$.

Hinton, and Ronald Williams in 1986 [104], but originally introduced by Paul Werbos in his 1974 Ph.D. thesis [105], allowed neural networks like the one shown in Fig. 6.1 to learn complex, non-linear patterns by adjusting the weights of the connections between layers. This breakthrough enabled the development of more powerful neural networks and expanded the scope of their applications.

## 6.2 Activation functions

Activation functions play a critical role in neural networks by introducing non-linear properties to the system. This non-linearity allows the network to learn from the error back-propagated and to perform tasks beyond just linear regression or classification. Mathematically, the activation function $f(x)$ operates on the weighted sum of the inputs $z$ at each neuron to produce an output $a$, which serves as the input for the next layer in the network. The process is represented as

$$a = f(z), \quad \text{where} \quad z = \sum_{i=1}^{n} w_i x_i + b. \tag{6.1}$$

Here, $w_i$ are weights associated with the connections between neurons, $x_i$ are the input features, $b$ is a bias term that allows the activation function to be shifted horizontally, and $z$ is the weighted linear combination of inputs. The output $a$, also known as the activation, is then forwarded to subsequent layers, where it serves as the input for the next layer of neurons.

Different types of activation functions like sigmoid, ReLU (rectified linear unit), and tanh (hyperbolic tangent) introduce different types of non-linearities into the system, as illustrated in Fig. 6.2. The choice of activation function can impact the efficiency of training, the convergence speed, and the performance of the neural network.

In the following subsections, we discuss some commonly used activation functions employed in neural networks, elaborating on their mathematical formulations and properties.

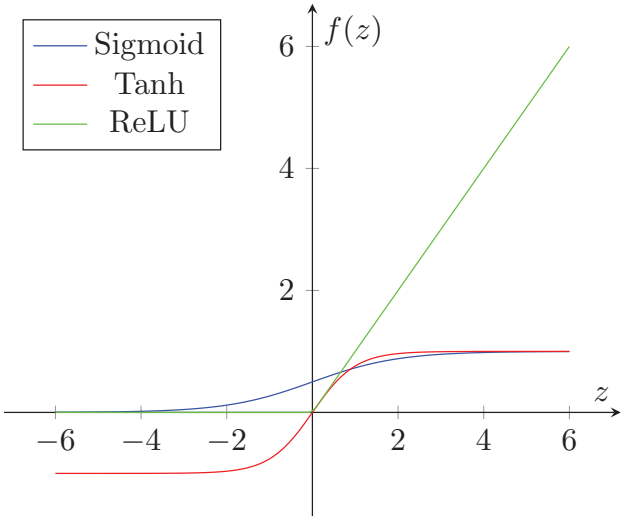


Figure 6.2: Common Activation Functions

**Sigmoid activation function**

The sigmoid activation function, also known as the logistic function, is defined mathematically by the equation

$$\sigma(x) = \frac{1}{1 + e^{-x}} \tag{6.2}$$

This function maps any input $x$ to a value between 0 and 1, thus providing a probabilistic interpretation. The sigmoid function is differentiable, and its derivative is given by

$$\sigma'(x) = \sigma(x) \cdot (1 - \sigma(x)) \tag{6.3}$$

Its derivative lies in the range $(0, 1)$, making it smooth and differentiable. The sigmoid function is often used in binary classification problems, as it outputs values that can be interpreted as probabilities. However, it suffers from vanishing-gradient problems when the input is either too large or too small, which can hinder learning in deep networks.

**Rectified linear unit (ReLU)**

The ReLU function is defined as

$$f(z) = \max(0, z) \tag{6.4}$$

ReLU has gained popularity for its computational efficiency and its ability to mitigate the vanishing-gradient problem, especially in deep networks.

In recent years, researchers have introduced these and other modifications to activation functions to further improve the adaptability and performance of neural networks.

**Hyperbolic tangent (tanh)**

The hyperbolic tangent function is defined as

$$f(z) = \tanh(z) = \frac{e^z - e^{-z}}{e^z + e^{-z}}. \tag{6.5}$$

The derivative of the tanh function lies in the range $(0, 0.25)$. Like the sigmoid, it is smooth and differentiable, but can suffer from vanishing gradients.

## 6.3 Learning rules in neural networks

In neural networks, learning rules guide the network to improve over time [106]. These rules adjust the internal parameters, known as weights and biases, during training. The main goal is to minimize a predefined metric called a "loss function," which quantifies the discrepancy between the network's predictions and the actual target values [107].

One of the most popular learning rules is gradient descent [108]. Imagine you are on a hill and aim to reach the bottom as quickly as possible but can only see a limited distance around you. Gradient descent is similar to choosing to walk in the direction where the hill slopes down the most. Mathematically, this involves updating the weights and biases to minimize the loss function. Each update is guided by the formula:

$$\text{New Setting} = \text{Old Setting} - (\text{Learning Speed} \times \text{Slope of the Hill}) \tag{6.6}$$

Here, "Learning Speed" is a hyperparameter that dictates the size of each step, and the "Slope of the Hill" is computed as the gradient of the loss function [109].

Gradient descent is favored because it is straightforward and versatile, capable of optimizing a variety of complex, high-dimensional functions [110]. It employs the gradient of the loss function to identify the most rapid descent direction, making it computationally efficient.

Several variants of basic gradient descent have been developed to enhance its efficacy. For instance:

- Stochastic gradient descent (SGD) employs smaller, more frequent updates using a subset of the data, thereby accelerating, but somewhat randomizing, the optimization process [111].
- 'Mini-batch gradient descent strikes a balance by using more data than SGD but fewer than the classic full-batch method [106].

More advanced optimization algorithms like Adam, RMSProp, and AdaGrad build on gradient descent by introducing adaptive learning rates and momentum, making the optimization landscape easier to navigate [112–114].

Choosing the appropriate learning rule and its variant is crucial for efficient and effective neural network training [106].

## 6.4 Types of neural networks

Feedforward neural networks (FNNs) [107], convolutional neural networks (CNNs) [115], recurrent neural networks (RNNs) [116], and Transformer networks [117] are among the most commonly used architectures in the field of neural networks. We tested several of them in Paper D for the task of identifying quantum advantage in random walks. Each network type has its own unique characteristics and best-use cases. The key differences between these network architectures is summarized in Table 6.1 [118, 119].

| **Type** | **Best For** | **Data Flow** | **Special Features** |
|---|---|---|---|
| FNN | General-Purpose | Feedforward | None |
| CNN | Image, Grid Data | Feedforward | Convolutional Layers |
| RNN | Sequence Data | Cyclic | Hidden State |
| Transformer | NLP Tasks | Feedforward | Self-Attention |

Table 6.1: Comparison of neural-network types.

# 7 Paper overview

This chapter aims to offer an exhaustive synthesis of the four cornerstone papers that collectively undergird the intellectual scaffolding of our research. It merits special attention that the papers appended herein are not solo endeavors but the fruits of concerted collaborative efforts. The pluralistic insights and specialized know-how contributed by multiple researchers have been instrumental in honing the theoretical paradigms expounded across these works.

## 7.1 Paper A — Gaussian conversion protocols for cubic phase state generation

In Paper A, we tackle a significant challenge in the realm of universal quantum computing with continuous variables: the creation of a cubic phase state (see Chapter 3.3), a non-Gaussian resource essential for such computing. Despite its theoretical importance, achieving a cubic phase state experimentally has been difficult. To overcome this, the paper introduces two Gaussian conversion protocols aimed at converting a trisqueezed state (see Chapter 3.2), which has been realized experimentally, into the elusive cubic phase state.

The first protocol is deterministic and employs active (inline) squeezing. After numerical optimization, we achieve fidelities of 0.971, which reach the theoretical upper limit for deterministic Gaussian protocols.

The second approach, described in Chapter 4.2 of this thesis, is probabilistic, leveraging an auxiliary squeezed state to eliminate the need for inline squeezing, while still, after optimization, yielding high probabilities of success and even greater fidelities. A fidelity as high as 0.997 can be achieved with a success probability of 5 %; the fidelity can be pushed above 0.999 if one is willing to accept a success probability of around 1 %.

These protocols, therefore, offer compelling evidence for the viability of using trisqueezed states as practical resources for universal quantum computing.

## 7.2 Paper B — Gaussian conversion protocol for heralded generation of generalized Gottesman– Kitaev–Preskill states

With Paper B, the thesis delves into the complex terrain of fault-tolerant quantum computing, focusing on the use of continuous-variable systems and bosonic codes for noise resilience. Bosonic codes, which map qubit-like quantum information onto a more expansive bosonic Hilbert space, come in two main types: translational-symmetric codes like GKP (Gottesman–Kitaev–Preskill) codes (see Chapter 3.5), and rotational-symmetric codes such as cat and binomial codes (see Chapter 3.4). The paper seeks to clarify the understood relationship between these two families of codes.

We introduce an iterative protocol capable of converting between GKP states and four-fold-symmetric binomial states, using only Gaussian operations. The protocol is described in Chapter 4.3. This groundbreaking conversion not only hints at the universal applicability of binomial states for all-Gaussian quantum computation but also paves the way for a new, heralded preparation technique for GKP states.

Numerical simulations reveal that GKP states (technically, generalized GKP states called qunaught states, which do not store quantum information but can be used to produce logical GKP states) with over 98 % fidelity and a success probability of around 3.14 % can be obtained in just two steps of the iterative process, although further iterations improve fidelity at the expense of success probability. The fall-off in success probability with more iterations is sharp: a slight increase in fidelity is only gained at the expense of orders of magnitude lower success probability.

We also show that binomial states with other parameters (rotational symmetry $N$ and truncation $K$; see Chapter 3.4) do not yield as high fidelities as the states with $N = 2$ and $K = 3$ that we focused our study on.

## 7.3 Paper C — Gaussian protocol for multimode states conversion

The study in Paper C expands the scope of research from the preceding two papers by introducing additional conversion protocols and investigating possible input and output states more systematically. The main contribution for this paper in this thesis is the protocol discussed in Chapter 4.4, which facilitates the generation of a two-photon state from separate one-photon states through the use of only Gaussian operations, thereby eliminating the need for photon-number detection, which is a non-Gaussian operation. It further demonstrates that wave packets are precisely matched in both spatial (mode matching) and temporal

dimensions for the generation of a two-photon state. With this protocol, we are able to generate a two-photon state with 0.99999 fidelity with a success probability exceeding 10 %. We also explored using many other input states for this protocol, but did not find such high fidelities for any other non-Gaussian target states.

## 7.4 Paper D — Detecting quantum speedup of random walks with machine learning

In Paper D, we investigate the potential of machine learning, particularly neural networks (see Chapter 6), for detecting quantum speedup in random walks on graphs (see Chapter 5). It evaluates the efficacy of three different neural-network architectures — variations of fully connected and convolutional networks — in identifying various types of graphs (linear, cyclic, and random) where quantum speedups manifest in hitting times. Hitting time refers to the time it takes to reach a specific target node after starting from another node in the graph.

In this study, we find that while carefully curating a good training-data set can improve neural-network performance, all tested architectures face difficulties in classifying large random graphs and generalizing their learning from one graph size to another. We speculate that a possible reason for this somewhat disappointing performance is that the neural networks can have trouble handling the sparse input data that is the adjacency matrix of the graph. Despite these limitations, the research suggests that if classification accuracy could be improved, neural networks may provide valuable insights into quantum advantage, not just in the context of random walks but also for broader applications in quantum computing and quantum transport.

# 8 Summary and outlook

In summary, this thesis encapsulates an in-depth exploration at the nexus of machine learning and quantum mechanics, featuring four papers that serve as its bedrock. These papers collectively address the utilization of machine learning and other optimization methods for identifying and transforming quantum resources across various applications.

The first three papers, A–C, dealt with conversion between resource states for CV quantum computation. Chapters 2–4 gave the background for this field, an overview of the resource states, and a description of the conversion protocols, respectively. Paper D investigated how neural networks, discussed in Chapter 6, perform on the task of classifying whether a quantum speed-up is possible compared to a classical random walk on a graph, described in Chapter 5.

The findings presented in this thesis pave the way for several promising avenues for future research:

- The observed challenge of low success rates in probabilistic Gaussian protocols, as highlighted in Papers A and B, opens up a fertile ground for further optimization. Potential solutions could be facilitated through advanced machine-learning algorithms.
- The groundbreaking revelation in Paper B, where binomial states were found to function as standalone quantum resources, raises intriguing questions about other states that could similarly serve this purpose.
- Paper C hints at the exciting possibility of generating complex multi-photon states via Gaussian operations. This warrants a detailed follow-up study to evaluate their potential utility in various quantum-computing architectures.
- The progress demonstrated in Paper D, where machine learning was employed to identify quantum advantage in random walks, suggests that further fine-tuning of neural networks could lead to more accurate predictions. This represents a compelling frontier for subsequent research.

In summary, this thesis not only broadens our understanding of the synergistic role machine learning can play in the discovery and optimization of quantum resources, but also sets the stage for pioneering advancements in the rapidly evolving field of quantum computing.

# Bibliography


[1] M. A. Nielsen and I. L. Chuang, *Quantum computation and quantum information* (Cambridge University Press, 2000).

[2] I. Georgescu, S. Ashhab, and F. Nori, Reviews of Modern Physics **86**, 153 (2014).

[3] C. Degen, F. Reinhard, and P. Cappellaro, Reviews of Modern Physics **89**, 035002 (2017).

[4] E. Chitambar and G. Gour, Reviews of Modern Physics **91**, 025001 (2019).

[5] A. Serafini, *Quantum continuous variables: a primer of theoretical methods* (CRC press, 2017).

[6] O. Pfister, Journal of Physics B: Atomic, Molecular and Optical Physics **53**, 012001 (2020).

[7] A. Blais, A. L. Grimsmo, S. M. Girvin, and A. Wallraff, Reviews of Modern Physics **93**, 025005 (2021).

[8] A. L. Grimsmo and A. Blais, npj Quantum Information **3**, 20 (2017).

[9] T. Hillmann, F. Quijandría, G. Johansson, A. Ferraro, S. Gasparinetti, and G. Ferrini, Physical Review Letters **125**, 160501 (2020).

[10] A. Joshi, K. Noh, and Y. Y. Gao, Quantum Science and Technology **6**, 033001 (2021).

[11] A. Serafini, A. Retzker, and M. B. Plenio, New Journal of Physics **11**, 023007 (2009).

[12] C. Flühmann, T. L. Nguyen, M. Marinelli, V. Negnevitsky, K. Mehta, and J. P. Home, Nature **566**, 513 (2019).

[13] M. Schmidt, M. Ludwig, and F. Marquardt, New Journal of Physics **14**, 125005 (2012).

[14] O. Houhou, H. Aissaoui, and A. Ferraro, Physical Review A **92**, 063843 (2015).

[15] W. H. P. Nielsen, Y. Tsaturyan, C. B. Møller, E. S. Polzik, and A. Schliesser, Proceedings of the National Academy of Sciences **114**, 62 (2017).

[16] J. Stasińska, C. Rodó, S. Paganelli, G. Birkl, and A. Sanpera, Physical Review A **80**, 062304 (2009).

[17] D. F. Milne and N. V. Korolkova, Physical Review A **85**, 032310 (2012).

[18] Y. Ikeda and N. Yamamoto, Physical Review A **87**, 033802 (2013).

[19] K. R. Motes, B. Q. Baragiola, A. Gilchrist, and N. C. Menicucci, Physical Review A **95**, 053819 (2017).

[20] M. V. Larsen, X. Guo, C. R. Breum, J. S. Neergaard-Nielsen, and U. L. Andersen, Science **366**, 369 (2019).

[21] W. Asavanant, Y. Shiozawa, S. Yokoyama, B. Charoensombutamon, H. Emura, R. N. Alexander, S. Takeda, J.-i. Yoshikawa, N. C. Menicucci, H. Yonezawa, and A. Furusawa, Science **366**, 373 (2019).

[22] F. Lenzini, J. Janousek, O. Thearle, M. Villa, B. Haylock, S. Kasture, L. Cui, H.-P. Phan, D. V. Dao, H. Yonezawa, P. K. Lam, E. H. Huntington, and M. Lobino, Science Advances **4**, eaat9331 (2018).

[23] J.-i. Yoshikawa, S. Yokoyama, T. Kaji, C. Sornphiphatphong, Y. Shiozawa, K. Makino, and A. Furusawa, APL Photonics **1**, 060801 (2016).

[24] A. Romanenko, R. Pilipenko, S. Zorzetti, D. Frolov, M. Awida, S. Belomestnykh, S. Posen, and A. Grassellino, Physical Review Applied **13**, 034032 (2020).

[25] D. Gottesman, A. Kitaev, and J. Preskill, Physical Review A **64**, 012310 (2001).

[26] N. C. Menicucci, Physical Review Letters **112**, 120504 (2014).

[27] P. Campagne-Ibarcq, A. Eickbusch, S. Touzard, E. Zalys-Geller, N. E. Frattini, V. V. Sivak, P. Reinhold, S. Puri, S. Shankar, R. J. Schoelkopf, L. Frunzio, M. Mirrahimi, and M. H. Devoret, Nature **584**, 368 (2020).

[28] J. Kempe, Contemporary Physics **44**, 307 (2003).

[29] K. Pearson, Nature **72**, 294 (1905).

[30] M. Kac, The American Mathematical Monthly **54**, 369 (1947).

[31] R. M. Nosofsky and T. J. Palmeri, Psychological Review **104**, 266 (1997).

[32] S. Brin and L. Page, Computer Networks and ISDN Systems **30**, 107 (1998).

[33] L. Grady, IEEE Transactions on Pattern Analysis and Machine Intelligence **28**, 1768 (2006).

[34] A. M. Childs, E. Farhi, and S. Gutmann, Physical Review A **65**, 012322 (2002).

[35] A. M. Childs, Physical Review Letters **102**, 180501 (2009).

[36] N. B. Lovett, S. Cooper, M. Everitt, M. Trevers, and V. Kendon, Physical Review A **81**, 042330 (2010).

[37] A. M. Childs, D. Gosset, and Z. Webb, Science **339**, 791 (2013).

[38] A. Peruzzo, M. Lobino, J. C. Matthews, N. Matsuda, A. Politi, K. Poulios, X.-Q. Zhou, Y. Lahini, N. Ismail, K. Wörhoff, *et al.*, Science **329**, 1500 (2010).

[39] H. Tang, X.-F. Lin, Z. Feng, J.-Y. Chen, J. Gao, K. Sun, C.-Y. Wang, P.-C. Lai, X.-Y. Xu, Y. Wang, L.-F. Qiao, A.-L. Yang, and X.-M. Jin, Science Advances **4**, eaat3174 (2018).

[40] C. Chen, X. Ding, J. Qin, Y. He, Y.-H. Luo, M.-C. Chen, C. Liu, X.-L. Wang, W.-J. Zhang, H. Li, L.-X. You, Z. Wang, D.-W. Wang, B. C. Sanders, C.-Y. Lu, and J.-W. Pan, Physical Review Letters **121**, 100502 (2018).

[41] Z. Yan, Y.-R. Zhang, M. Gong, Y. Wu, Y. Zheng, S. Li, C. Wang, F. Liang, J. Lin, Y. Xu, C. Guo, L. Sun, C.-Z. Peng, K. Xia, H. Deng, H. Rong, J. Q. You, F. Nori, H. Fan, X. Zhu, and J.-W. Pan, Science **364**, 753 (2019).

[42] M. Gong, S. Wang, C. Zha, M.-C. Chen, H.-L. Huang, Y. Wu, Q. Zhu, Y. Zhao, S. Li, S. Guo, H. Qian, Y. Ye, F. Chen, C. Ying, J. Yu, D. Fan, D. Wu, H. Su, H. Deng, H. Rong, K. Zhang, S. Cao, J. Lin, Y. Xu, L. Sun, C. Guo, N. Li, F. Liang, V. M. Bastidas, K. Nemoto, W. J. Munro, Y.-H. Huo, C.-Y. Lu, C.-Z. Peng, X. Zhu, and J.-W. Pan, Science **372**, 948 (2021).

[43] A. W. Young, W. J. Eckner, N. Schine, A. M. Childs, and A. M. Kaufman, Science **377**, 885 (2022).

[44] S. Lloyd and S. L. Braunstein, Physical Review Letters **82**, 1784 (1999).

[45] A. Ferraro, S. Olivares, and M. G. A. Paris, Gaussian states in continuous variable quantum information (2005), arXiv:quant-ph/0503237 .

[46] C. Weedbrook, S. Pirandola, R. García-Patrón, N. J. Cerf, T. C. Ralph, J. H. Shapiro, and S. Lloyd, Reviews of Modern Physics **84**, 621 (2012).

[47] G. Adesso, S. Ragy, and A. R. Lee, Open Systems & Information Dynamics **21**, 1440001 (2014).

[48] F. Albarelli, M. G. Genoni, M. G. A. Paris, and A. Ferraro, Physical Review A **98**, 052350 (2018).

[49] R. Takagi and Q. Zhuang, Physical Review A **97**, 062337 (2018).

[50] B. Q. Baragiola, G. Pantaleoni, R. N. Alexander, A. Karanjai, and N. C. Menicucci, Physical Review Letters **123**, 200502 (2019).

[51] H. Yamasaki, T. Matsuura, and M. Koashi, Physical Review Research **2**, 023270 (2020).

[52] M. Gu, C. Weedbrook, N. C. Menicucci, T. C. Ralph, and P. Van Loock, Physical Review A **79**, 062318 (2009).

[53] T. Douce, D. Markham, E. Kashefi, P. van Loock, and G. Ferrini, Physical Review A **99**, 012344 (2019).

[54] A. Ambainis, E. Bach, A. Nayak, A. Vishwanath, and J. Watrous, in *Proceedings of the thirty-third annual ACM symposium on Theory of computing* (ACM, New York, NY, USA, 2001) pp. 37–49.

[55] D. Aharonov, A. Ambainis, J. Kempe, and U. Vazirani, in *Proceedings of the thirty-third annual ACM symposium on Theory of computing* (ACM, New York, NY, USA, 2001) pp. 50–59.

[56] A. M. Childs, R. Cleve, E. Deotto, E. Farhi, S. Gutmann, and D. A. Spielman, in *Proceedings of the thirty-fifth annual ACM symposium on Theory of computing* (ACM, New York, NY, USA, 2003) pp. 59–68.

[57] J. Kempe, Probability Theory and Related Fields **133**, 215 (2005).

[58] D. Solenov and L. Fedichkin, Physical Review A **73**, 012313 (2006).

[59] H. Krovi and T. A. Brun, Physical Review A **73**, 032341 (2006).

[60] R. A. M. Santos and R. Portugal, International Journal of Quantum Information **08**, 881 (2010).

[61] A. Makmal, M. Zhu, D. Manzano, M. Tiersch, and H. J. Briegel, Physical Review A **90**, 022314 (2014).

[62] V. Gualtieri, C. Benedetti, and M. G. A. Paris, Physical Review A **102**, 012201 (2020).

[63] S. Chakraborty, L. Novo, and J. Roland, Physical Review A **102**, 032214 (2020).

[64] S. Balasubramanian, T. Li, and A. Harrow, Exponential speedups for quantum walks in random hierarchical graphs (2023), arXiv:2307.15062 .

[65] M. H. Michael, M. Silveri, R. T. Brierley, V. V. Albert, J. Salmilehto, L. Jiang, and S. M. Girvin, Physical Review X **6**, 031006 (2016).

[66] C. K. Andersen, A. Remm, S. Lazar, S. Krinner, N. Lacroix, G. J. Norris, M. Gabureac, C. Eichler, and A. Wallraff, Nature Physics **16**, 875 (2020).

[67] K. Fukui and S. Takeda, Journal of Physics B: Atomic, Molecular and Optical Physics **55**, 012001 (2022).

[68] S. L. Braunstein and P. van Loock, Reviews of Modern Physics **77**, 513 (2005).

[69] C. Gerry, P. Knight, and P. L. Knight, *Introductory quantum optics* (Cambridge university press, 2005).

[70] W. Heisenberg, Zeitschrift für Physik **43**, 172 (1927).

[71] W. B. Case, American Journal of Physics **76**, 937 (2008).

[72] R. Hudson, Reports on Mathematical Physics **6**, 249 (1974).

[73] S. D. Bartlett, B. C. Sanders, S. L. Braunstein, and K. Nemoto, Physical Review Letters **88**, 097904 (2002).

[74] A. Mari and J. Eisert, Physical Review Letters **109**, 230503 (2012).

[75] V. Veitch, C. Ferrie, D. Gross, and J. Emerson, New Journal of Physics **14**, 113011 (2012).

[76] A. Kenfack and K. Yczkowski, Journal of Optics B: Quantum and Semiclassical Optics **6**, 396 (2004).

[77] N. C. Menicucci, S. T. Flammia, and P. van Loock, Physical Review A **83**, 042335 (2011).

[78] S. Takeda, T. Mizuta, M. Fuwa, P. van Loock, and A. Furusawa, Nature Photonics **7**, 982 (2013).

[79] R. Jozsa, in *Quantum Information Processing – From Theory to Experiment*, NATO Science Series, III: Computer and Systems Sciences, Vol. 199 (2006) pp. 137–158.

[80] D. Gottesman and I. L. Chuang, Nature **402**, 390 (1999).

[81] G. De Palma, A. Mari, V. Giovannetti, and A. S. Holevo, Journal of Mathematical Physics **56**, 052202 (2015).

[82] C. K. Hong, Z. Ou, and L. Mandel, Physical Review Letters **59**, 2044 (1987).

[83] S. Haroche and J.-M. Raimond, *Exploring the Quantum: Atoms, Cavities, and Photons* (Oxford University Press, Oxford, 2006).

[84] P. Maunz, D. L. Moehring, S. Olmschenk, K. C. Younge, D. N. Matsukevich, and C. Monroe, Nature Physics **3**, 538 (2007).

[85] S. L. Braunstein and R. I. McLachlan, Physical Review A **35**, 1659 (1987).

[86] K. Banaszek and P. L. Knight, Physical Review A **55**, 2368 (1997).

[87] V. V. Albert and L. Jiang, Physical Review A **89**, 022118 (2014).

[88] D. Stahlke, Physical Review A **90**, 022302 (2014).

[89] M. H. Michael, M. Silveri, R. Brierley, V. V. Albert, J. Salmilehto, L. Jiang, and S. Girvin, Physical Review X **6**, 031006 (2016).

[90] D. Gottesman, A. Kitaev, and J. Preskill, Physical Review A **64**, 012310 (2001).

[91] W. Cai, Y. Ma, W. Wang, C.-L. Zou, and L. Sun, Fundamental Research **1**, 50 (2021).

[92] V. V. Albert, K. Noh, K. Duivenvoorden, D. J. Young, R. T. Brierley, P. Reinhold, C. Vuillot, L. Li, C. Shen, S. M. Girvin, B. M. Terhal, and L. Jiang, Physical Review A **97**, 032346 (2018).

[93] K. Duivenvoorden, B. M. Terhal, and D. Weigand, Physical Review A **95**, 012305 (2017).

[94] D. J. Weigand and B. M. Terhal, Physical Review A **97**, 022341 (2018).

[95] L. Lovász, *Random Walks on Graphs: A Survey* (Springer, 1993).

[96] J. R. Norris, *Markov Chains* (Cambridge University Press, 1998).

[97] N. Masuda, M. A. Porter, and R. Lambiotte, Physics Reports **716-717**, 1–58 (2017).

[98] D. Aldous and J. A. Fill, *Reversible Markov Chains and Random Walks on Graphs* (1999).

[99] D. J. Watts, *Small worlds: the dynamics of networks between order and randomness* (Princeton University Press, 2004).

[100] A. A. Melnikov, L. E. Fedichkin, and A. Alodjants, AIP Conference Proceedings **2241**, 020029 (2020).

[101] A. A. Melnikov, L. E. Fedichkin, and A. Alodjants, New Journal of Physics **21**, 125002 (2019).

[102] W. S. McCulloch and W. Pitts, The Bulletin of Mathematical Biophysics **5**, 115 (1943).

[103] F. Rosenblatt, Psychological Review **65**, 386 (1958).

[104] D. E. Rumelhart, G. E. Hinton, and R. J. Williams, Nature **323**, 533 (1986).

[105] P. J. Werbos, *Beyond Regression: New Tools for Prediction and Analysis in the Behavioral Sciences*, Ph.D. thesis, Harvard University (1974).

[106] I. Goodfellow, Y. Bengio, and A. Courville, *Deep Learning* (MIT Press, 2016).

[107] C. M. Bishop, *Pattern Recognition and Machine Learning* (Springer, 2006).

[108] S. Ruder, An overview of gradient descent optimization algorithms (2016), arXiv:1609.04747 .

[109] L. Bottou, in *The 22nd International Conference on Artificial Intelligence and Statistics* (2018) pp. 171–172.

[110] Y. LeCun, Y. Bengio, and G. Hinton, Nature **521**, 436 (2015).

[111] L. Bottou, in *Proceedings of COMPSTAT'2010* (Springer, 2010) pp. 177–186.

[112] D. P. Kingma and J. Ba, in *International Conference on Learning Representations* (2014).

[113] T. Tieleman and G. Hinton, Rmsprop and equilibrated adaptive learning rates for non-convex optimization (2012).

[114] J. Duchi, E. Hazan, and Y. Singer, in *Journal of Machine Learning Research* (2011) pp. 2121–2159.

[115] Y. LeCun, L. Bottou, Y. Bengio, and P. Haffner, Proceedings of the IEEE **86**, 2278 (1998).

[116] J. L. Elman, Cognitive Science **14**, 179 (1990).

[117] N. Parmar and I. Bello, arXiv preprint arXiv:2101.01169 (2021).

[118] I. Goodfellow, Y. Bengio, and G. Hinton, Nature **521**, 436 (2015).

[119] Z. Zhang, Y. Zhao, and J. Wang, Artificial Intelligence Review **53**, 4035 (2020).